Electronic Supplementary Material (ESI) for Energy & Environmental Science.
This journal is © The Royal Society of Chemistry 2020

**Supporting Information**

# Insights into the Carbon Balance for $CO_2$ Electroreduction on Cu using Gas Diffusion Electrode Reactor Designs

Ming Ma,[†] Ezra L. Clark,[†] Kasper T. Therkildsen,[‡] Sebastian Dalsgaard,[†] Ib Chorkendorff[†] and Brian Seger[†,*]

[†]Surface Physics and Catalysis (Surfcat) Section, Department of Physics, Technical University of Denmark, 2800 Kgs Lyngby, Denmark

[‡]Siemens A/S, RC-DK SI, Diplomvej 378, 2800 Kgs. Lyngby, Denmark

*Author to whom correspondence should be addressed.

E-mail address: brse@fysik.dtu.dk

Tel.: +45 45253174

## Materials

Potassium bicarbonate ($KHCO_3$, ≥99.95%) and potassium hydroxide hydrate ($NaOH \cdot xH_2O$, 99.995%, Suprapur®) were purchased from Sigma Aldrich. All chemicals were used in this study without further purification. Anion exchange membrane (AEM, Fumasep FAA-3-PK-75) and gas-diffusion electrode (GDE, Sigracet 39 BC) were purchased from Fuel Cell Store. Iridium dioxide ($IrO_2$) purchased from Dioxide Materials was used as anode in $CO_2$ flow electrolyzers.

## Catalysts fabrication and characterization

In this work, Cu catalsyts were deposited on the top of microporous layer of gas-diffusion electrodes by direct current magnetron sputtering from a Cu target. In order to obtain the accurate deposition rate of Cu, Cu films were deposited on Si substrates, and then the cross-sectional SEM of Cu film/Si was peformed. Figure S1 shows the cross-sectional SEM image of Cu film/Si deposited for 50 min, which indicates the fact that ~200 nm thick Cu film was synthesized, corresponding to a Cu depositon rate of ~4 nm/min.

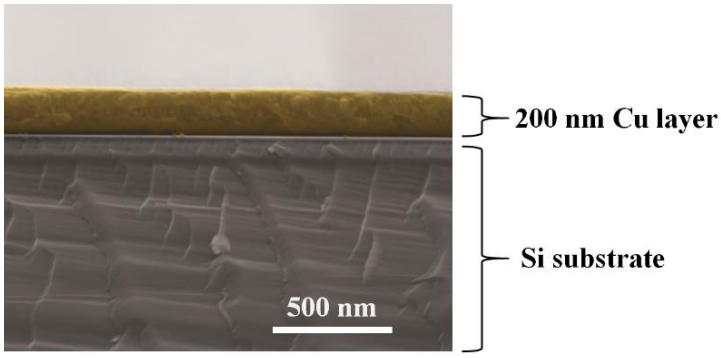


Figure S1. Cross-sectional SEM image of Cu layer deposited on Si by magnetron sputtering for 50 min.

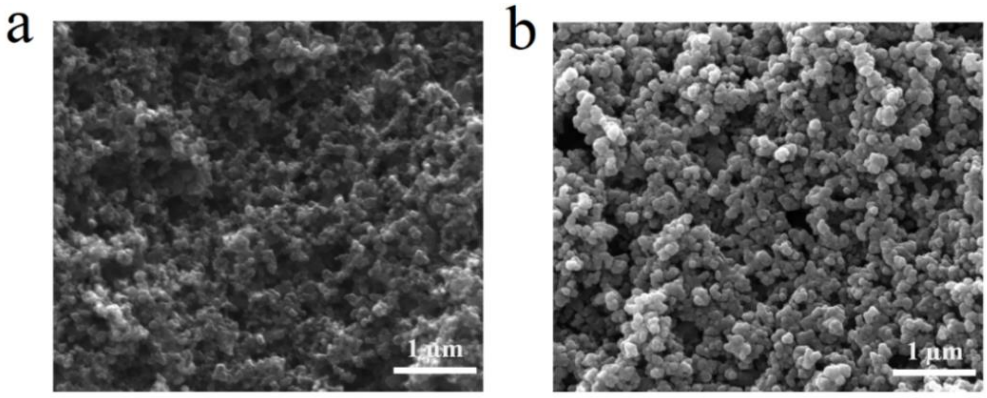


Figure S2. SEM images of microporous carbon layers (a) of gas-diffusion electrodes and Cu catalysts (b) coated on microporous carbon layers of gas-diffusion electrodes.

Figure S3. Digital image of Cu deposited on a gas-diffusion electrode.

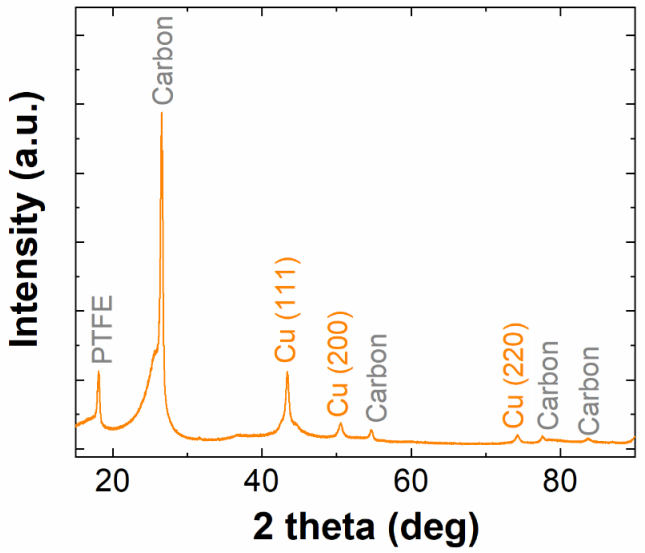


Figure S4. XRD patterns of Cu coated on a gas-diffusion electrode (Sigracet 39 BC). XRD measurements were performed using Cu Kα radiation.

**Faradaic efficiency calculation**

The Faradaic efficiency (FE) of product can be calculated according to the below equation:

$$FE\ (\%) = \frac{Q_{product}}{Q_{tot}} \times 100\% \qquad (S1)$$

where $Q_{product}$ and $Q_{tot}$ are charge transferred for product formation and charge passed through the working electrode, respectively.

Based on the above equation, the detailed caculation for Faradaic efficiency of gas product could be written as:

$$FE\ (\%) = \frac{n \times C_{product} \times \emptyset t \times \frac{P_o}{RT} \times F}{I \times t} \times 100\% \qquad (S2)$$

where $C_{product}$ and n are the concentration of gas product measured by GC and the number of electrons required for producing one molecule of the related gas product, respectively. $\emptyset$ is gas flow rate, $t$ is the electrolysis time, $P_o$ is ambient pressure, $F$ is Faraday constant, , $R$ is ideal gas constant, T is absolute temperature, and $I$ is current.

## High local pH at cathode/electrolyte interface

In the electrocatalytic $CO_2$ reduction process, $CO_2$ can be converted into a variety of gas and liquid products when combined with water on metal surfaces in aqueous solutions according to the reactions[1–3]:

$$CO_2 + H_2O + 2e^- \rightarrow CO + 2OH^- \quad \text{(-0.11 V vs. RHE)} \quad \text{(S3)}$$

$$CO_2 + 6H_2O + 8e^- \rightarrow CH_4 + 8OH^- \quad \text{(0.17 V vs. RHE)} \quad \text{(S4)}$$

$$2CO_2 + 8H_2O + 12e^- \rightarrow C_2H_4 + 12OH^- \quad \text{(0.08 V vs. RHE)} \quad \text{(S5)}$$

$$CO_2 + H_2O + 2e^- \rightarrow HCOO^- + OH^- \quad \text{(-0.03 V vs. RHE)} \quad \text{(S6)}$$

$$CO_2 + 5H_2O + 6e^- \rightarrow CH_3OH + 6OH^- \quad \text{(0.03 V vs. RHE)} \quad \text{(S7)}$$

$$2CO_2 + 9H_2O + 12e^- \rightarrow C_2H_5OH + 12OH^- \quad \text{(0.09 V vs. RHE)} \quad \text{(S8)}$$

The competing $H_2$ evolution is an unavoidable reaction in $CO_2$ electroreduction. Thus, water is reduced to $H_2$ on the surface of catalyst according to the reaction[1]:

$$2H_2O + 2e^- \rightarrow H_2 + 2OH^- \quad \text{(0 V vs. RHE)} \quad \text{(S9)}$$

Thus, $OH^-$ ions are produced at the cathode/electrolyte interface in the cathodic reactions (Equation (3-9)), leading to an increased pH near the surface of cathode.[2,3]

## Reaction of $CO_2$ and $OH^-$ near cathode surface

In addition to the electrochemcial $CO_2$ reduction, $CO_2$ also can react with $OH^-$ created at the electrode/electrolyte interface by cathodic reactions (Equation (S3-S9)) using $KHCO_3$ electrolye in our three-compartment flow electrolyzer. Of particular note, $CO_2$ not only reacts with $OH^-$ generated by cathodic reactions (Equation (S3-S9)) but also reacts with $OH^-$ derived from electrolyte during $CO_2$ electroreduction in KOH solutions.

## $CO_2$ reduction and flowrate mesurement of gas outlet after cell

The electroreduction of $CO_2$ was conducted in a three-compartment flow electrolyzer made from Teflon at ambient temperature and pressure. In the cell, catholyte and anolyte flow compartments are separated by an anion exchange membrane, along with continuous flow electrolyte (each bottle is filled with 50 ml electrolyte), as shown in Figure S5. In addition, $CO_2$ was fed into gas chamber at a constant flowrate of 45 ml/min, and then gaseous $CO_2$ could pass through the gas-diffusion layer, diffusing into the surface of the catalyst which was immesed into electrolyte.

During the electroreduction of $CO_2$, the gas mixture (gas outlet) after reactor was directly vented into the gas-sampling loop of a GC for periodic quantificaiton of gas products. In order to get the reliable Faradaic efficiency of gas prouduts, the volumetric flowrate of gas outlet (gas mixture) after reactor was also measured by flow meter during the $CO_2$ reduction, as displayed in Figure S5. Gas outlet flowrate from the gas chamber after $CO_2$ reduction was plotted at various current densities for 1 M $KHCO_3$, 1 M KOH and 5 M KOH electrolyte, respectively (Figure S6). As noted in Figure S6, an obvious decrement in the flowrate of outlet was detected with increasing current densities in the same electrolyte. Here, we calculated the decrease rate of outlet flowrate as a function of current density in 1 M $KHCO_3$, 1 M KOH and 5 M KOH electrolyte, respectively (slope values in Figure S6).

In addition, gas outlet flowrate (or $CO_2$ consumption) should also be correlated with the surface area of Cu coated on GDE. Thus, a fixed geometric surface area (2 $cm^2$) of Cu layer was utilized for all the experiments in this study.

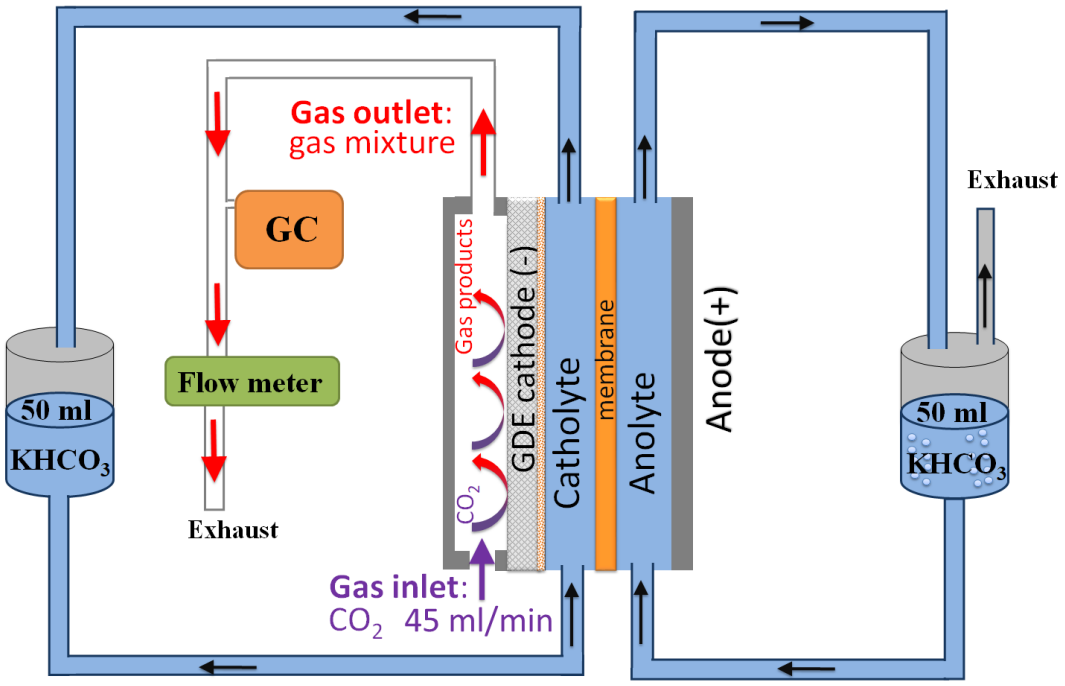


Figure S5. The schematic illustration of flow cell setup for reduction of $CO_2$.

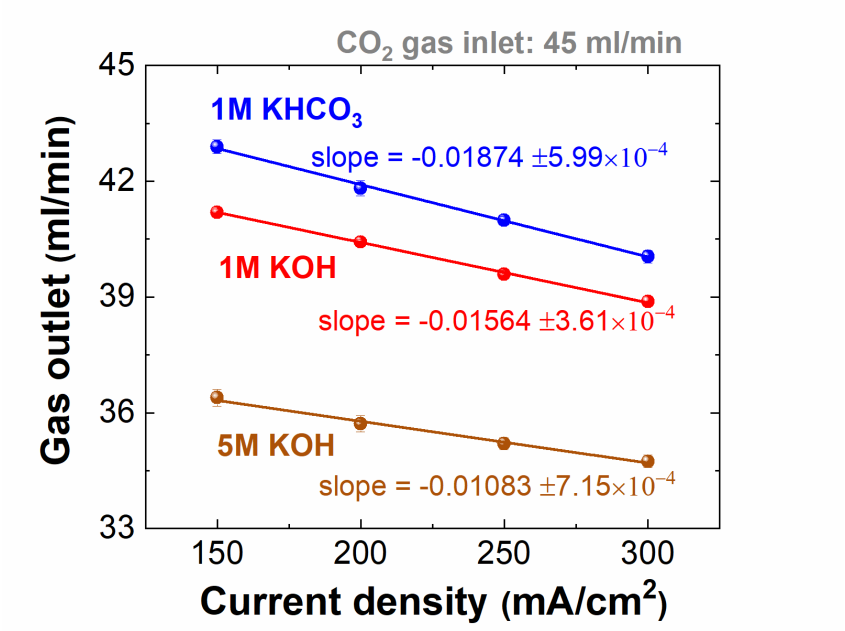


Figure S6. Gas outlet flowrates from the gas chamber after $CO_2$ reduction at various current densities in 1 M $KHCO_3$ (pH 8.33), 1 M KOH (pH 13.61) and 5 M KOH electrolyte, respectively (geometric surface area of Gu layer on GDE is 2 $cm^2$).

## $CO_2$ reduction performance

Based on the aforementioned flowrate measurement, the volumetric flowrate of gas outlet (gas mixture) after reactor was mornitored by flow meter in the course of the $CO_2$ reduction, and then Faradaic efficiencies of gas products were calcuated based on the mornitored outlet flowrate. Figure S7 shows the typical catalytic selectivity of gas products over time in 1 M $KHCO_3$ (a) and 1 M KOH (b) at 200 mA/cm$^2$, respectivily. The average catalytic selevitity of gas products in Figure 2 was taken during 2.5 h $CO_2$ reduction electrolysis with the exception of 5 M KOH (fast catalytic deactivation occurred in 5 M KOH due to GDEs lost hydrophobicity during operation in extremely high concentration of KOH[4]).

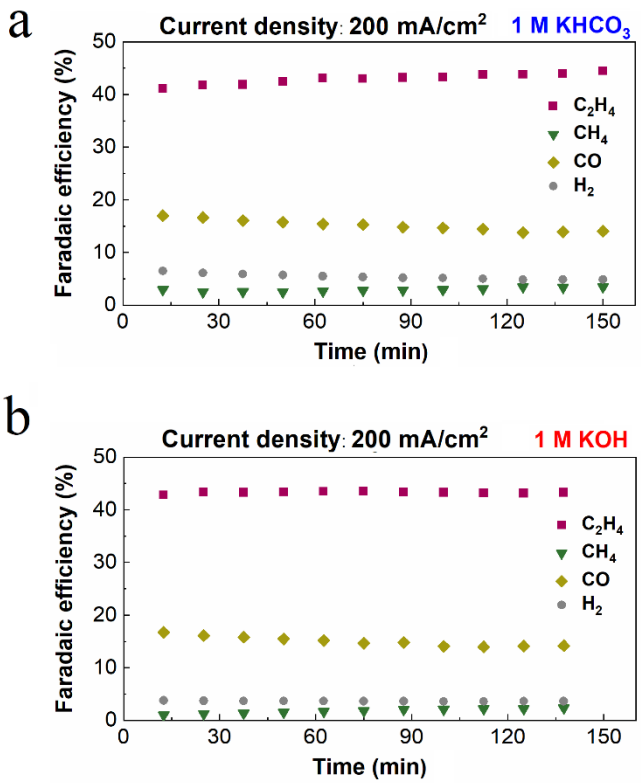


Figure S7. Catalytic selectivity of gas products over Cu catalylsts in 1 M $KHCO_3$ (a) and 1 M KOH (b) at 200 mA/cm$^2$, respectivily. All the tests were performed using 70 nm Cu layer coated on GDEs.

## Analysis of gas released from anolyte

$CO_2$ reduction with the competing $H_2$ evolution takes place on the surface of cathode while $O_2$ evolution happens on the anode surface. Interestingly, $H^+$ created at the anode/electrolyte interface by anodic reaction (Equation 3) could be neutralized by $HCO_3^-$ or $CO_3^{2-}$ after using $KHCO_3$ electrolyte. According to the reactions (Equation 7-8), gaseous $CO_2$ should be also released from $KHCO_3$ anolyte, accompanying with $O_2$. The flow cell setup for reduction of $CO_2$ in Figure S8 was used to analyse the gases released from anolyte. Specifically, gases released from anolyte were diluted with $N_2$ carrier gas at a constant flowrate, and then directly went into the gas sampling-loop of the GC to quantify the gases periodically. In addition, the volumetric gas flowrate released from anolyte was also mornitored by flow meter over the $CO_2$ reduction electrolysis (Figure S8).

After using 1 M $KHCO_3$ as electrolyte for $CO_2$ reduction, $CO_2$ released from anolyte was detected via GC, accompanying with $O_2$ at various current densities (Figure S9). In addition, the related $CO_2/O_2$ ratio released from anolyte over $CO_2$ reduction electrolysis at current densities of 150 mA/cm$^2$, 250 mA/cm$^2$, 300 mA/cm$^2$ using 1 M $KHCO_3$ as the initial catholyte and anolyte was also presented in Figure S9.

In contrast, only $O_2$ (~1.5 ml/min) was detected from anolyte at 200 mA/cm$^2$ over 6 h electrolysis after using 1 M KOH (Figure S11), due to a slow transition of electrolyte caused by the large amount of KOH (each bottle was filled with 50 ml 1 M KOH as initial catholyte and anolyte). For observing a relatively rapid electrolyte transition, each bottle (initial catholyte and anolyte) was filled with 20 ml 1 M KOH, discovering the initial $CO_2$ generation from anolyte after 2.5 h electrolysis, as shown in Figure 6.

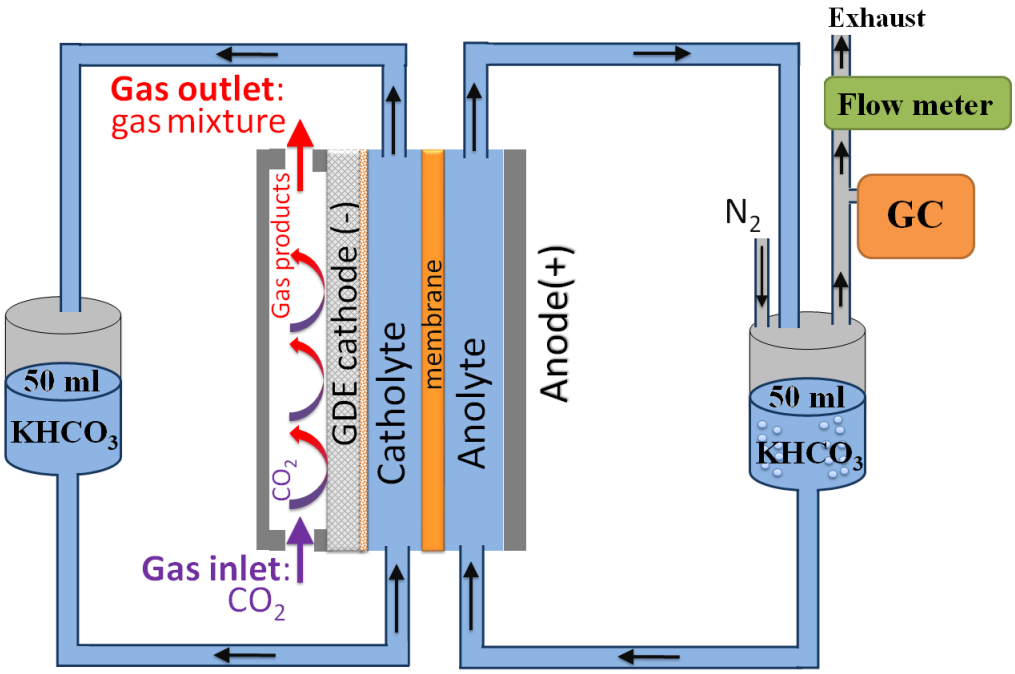


Figure S8. The schematic illustration of flow cell setup for analysing gases released from anolyte during $CO_2$ reduction.

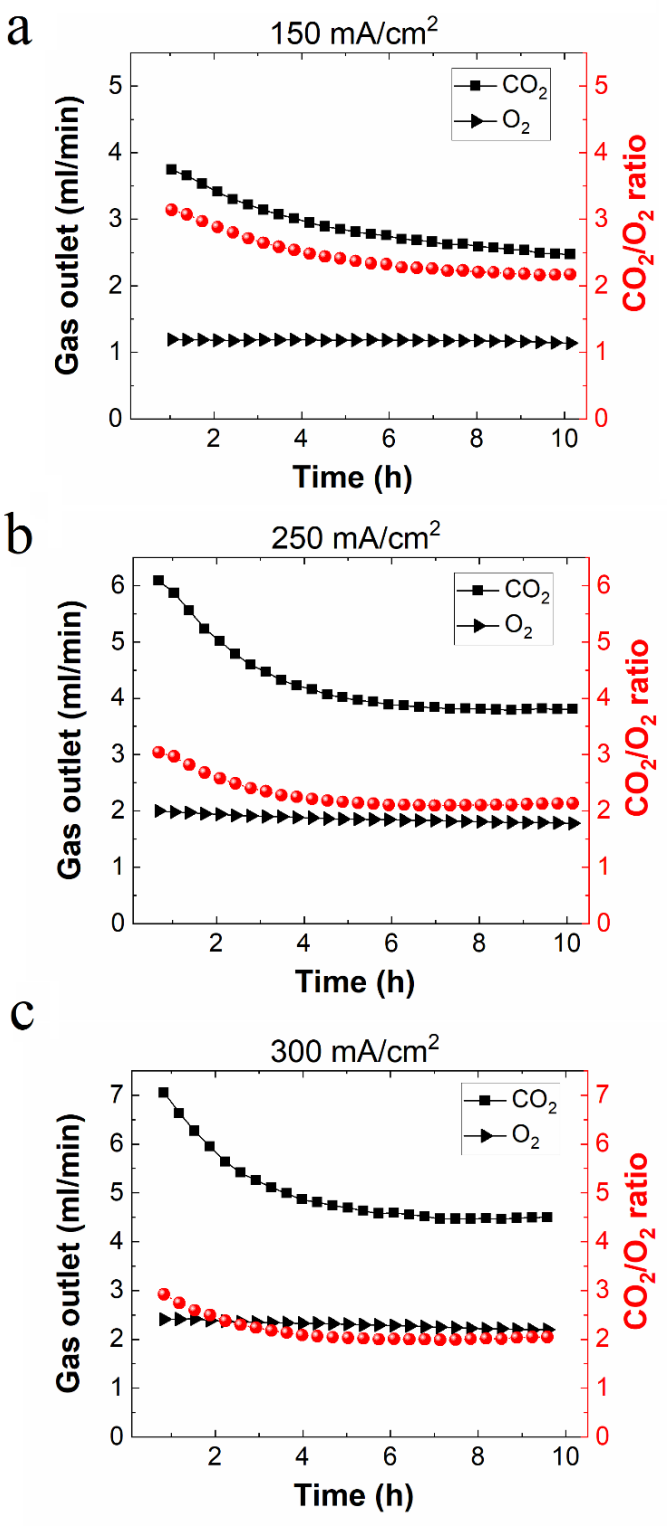


Figure S9. The flowrate of $O_2$ and $CO_2$ released from anolyte and the related $CO_2/O_2$ ratio over $CO_2$ reduction electrolysis at current densities of (a) 150 mA/cm$^2$, (b) 250 mA/cm$^2$, (c) 300 mA/cm$^2$ using 1 M $KHCO_3$ as the initial catholyte and anolyte (each both was filled with 50 ml 1 M $KHCO_3$ electrolyte).

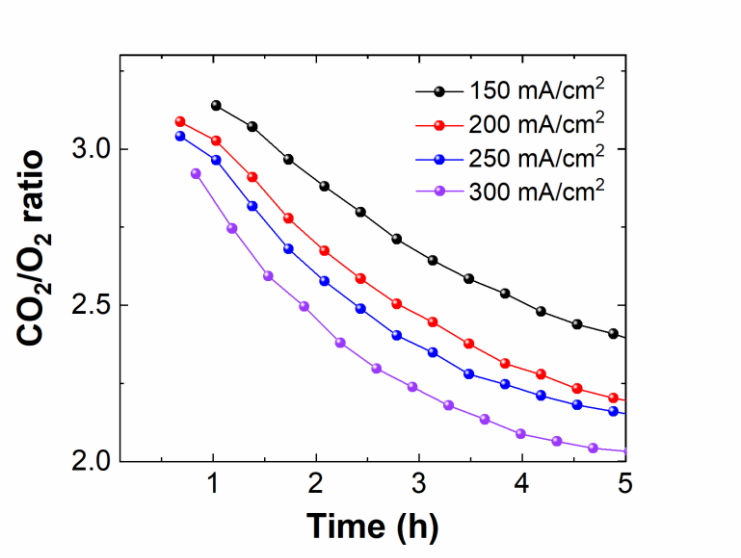


Figure S10. $CO_2/O_2$ flowrate ratio released from anolyte as a function of time at various current densities after using 1 M $KHCO_3$ as the initial catholyte and anolyte (each bottle was filled with 50 ml 1 M $KHCO_3$ electrolyte).

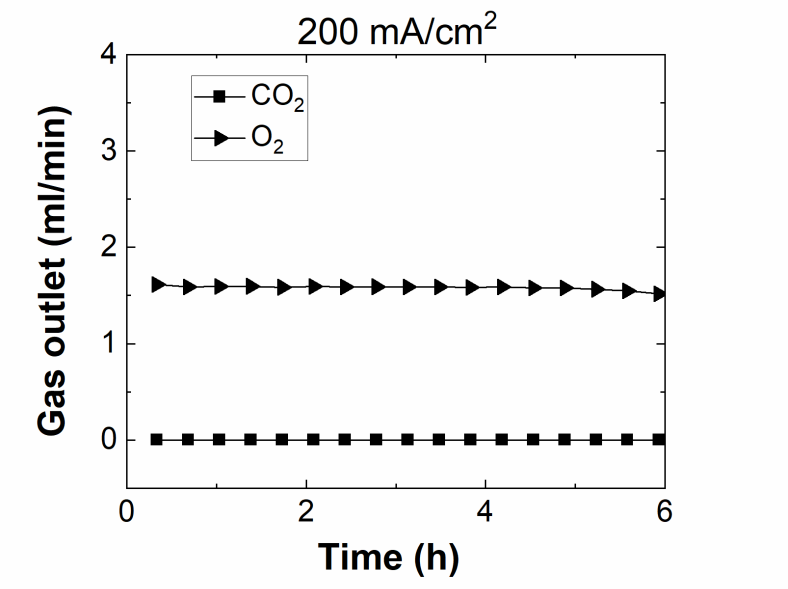


Figure S11. The flowrate of $O_2$ and $CO_2$ released from anolyte over $CO_2$ reduction electrolysis in 1 M KOH (each bottle was filled with 50 ml 1 M KOH as initial catholyte and anolyte).

**Theoretical $O_2$ and $CO_2$ flowrate released from anolyte**

If charge passed through anode is only used for $O_2$ evolution reaction, $O_2$ flowrate released in anolyte can be expressed as:

$$\emptyset\ (O_2) = \frac{Q_{tot}}{nF} \times \frac{RT}{P_o} \qquad (S10)$$

where $Q_{tot}$ and n are charge passed through the anode electrode and the number (here is 4) of holes required for producing one $O_2$ molecule, respectively. *F* is Faradaic constant, *R* is ideal gas constant, T is absolute temperature, and $P_o$ is ambient pressure.

If bicarbonate or carbonate is the only charge-carrier via anion exhange membrane, the $CO_2$ flowrate should be $4 \times \emptyset\ (O_2)$ and $2 \times \emptyset\ (O_2)$ according to the Equation (7) and Equation (8), respectively. Based on these equations, the flowrates for $CO_2$ and $O_2$ were calculated at various current densities (electrode surface area is 2 $cm^2$), as shown in Figure S12.

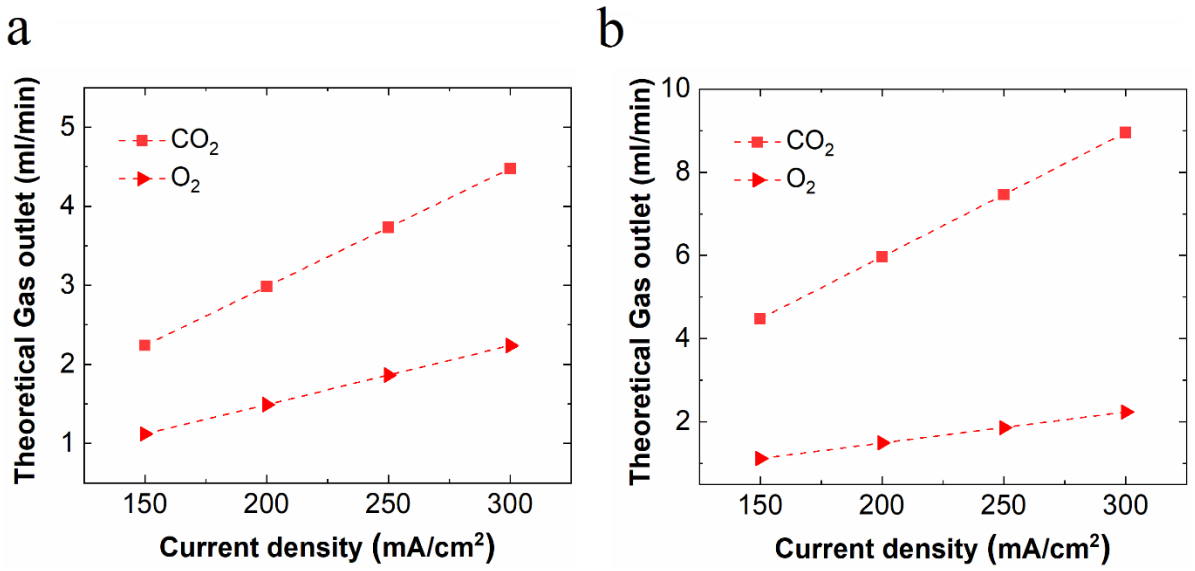


Figure S12. The estimated flowrates of $O_2$ and $CO_2$ released from anolyte as a function of current density based on the assumption of that the only charge-carrier via AEM is carbonate (a) or bicarbonate (b).

**Carbon balance calculation**

The unreacted $CO_2$ (residual $CO_2$) flowrate in the gas outlet (gas mixture) after reactor can be expressed as:

$$\emptyset_{residual\ CO_2} = \emptyset_{outlet} - (\emptyset_{CO} + \emptyset_{CH_4} + \emptyset_{C_2H_4} + \emptyset_{H_2}) \quad (S11)$$

where $\emptyset_{outlet}$ is the flowrate of gas outlet from the gas chamber after $CO_2$ reduction. $\emptyset_{CO}$, $\emptyset_{CH_4}$, $\emptyset_{C_2H_4}$ and $\emptyset_{H_2}$ are the gas flowrate of CO, $CH_4$, $C_2H_4$ and $H_2$ in the gas outlet from gas chamber during electrolysis, respectively.

The consumed $CO_2$ flowrate which is electrochemcially converted into all gas products (CO, $C_2H_4$ and $CH_4$) can be written as:

$$\emptyset_{CO_2\ to\ gas} = \emptyset_{CO} + \emptyset_{CH_4} + 2\emptyset_{C_2H_4} \quad (S12)$$

The consumed $CO_2$ flowrate for electrocatalytic reduction to all liquid products (such as ethanol and formate) can be written as:

$$\emptyset_{CO_2\ to\ liquid} = \emptyset_{C_1} + \emptyset_{C_2} + \emptyset_{C_3} \quad (S13)$$

where $\emptyset_{C_1}$, $\emptyset_{C_2}$, and $\emptyset_{C_3}$ are the consumed $CO_2$ flowrate for forming $C_1$, $C_2$ and $C_3$ liquid products, respectively.

$CO_2$ reduction at high reaction rates, $CO_2$ conversion into gas products (> $C_1$) and liquid products could reduce the gas outlet flowrate. In addition, the $CO_2$ consumption at high current via the reaction between $OH^-$ and $CO_2$ could significantly contribute to the decrease of the total gas outlet flowrate (Figure S6). Thus, the carbon element from $CO_2$ inlet flowrate should be eventually balanced by the below equation:

$$\emptyset_{inlet\ CO_2} = \emptyset_{residual\ CO_2} + \emptyset_{CO_2\ to\ gas} + \emptyset_{CO_2\ to\ liquid} + \emptyset_{OH^-} \quad (S14)$$

where $\emptyset_{OH^-}$ is the consumed $CO_2$ flowrate via the reaction with $OH^-$ (Equation 1 or 2).

**Table S1**. Carbon balance and related $CO_2$ utilization rate (ratio of $CO_2$ used in products formation to total $CO_2$ consumption) in 1 M $KHCO_3$.

| J ($mA/cm^2$) | $\emptyset_{CO_2\ to\ gas}$ (ml/min) | $\emptyset_{CO_2\ to\ liquid}$ (ml/min) | $\emptyset_{OH^-}$ (ml/min) | $\emptyset_{residual\ CO_2}$ (ml/min) | $CO_2$ utilization rate (%) |
|---|---|---|---|---|---|
| 150 | 0.749 | 0.267 | 2.4898 | 42.0 | 29.0 |
| 200 | 0.922 | 0.371 | 3.11156 | 40.8 | 29.4 |
| 250 | 1.169 | 0.4226 | 3.80596 | 39.735 | 29.5 |
| 300 | 1.379 | 0.516 | 4.50385 | 38.616 | 29.6 |

**Table S2**. Carbon balance and related $CO_2$ utilization rate in1 M KOH.

| J ($mA/cm^2$) | $\emptyset_{CO_2\ to\ gas}$ (ml/min) | $\emptyset_{CO_2\ to\ liquid}$ (ml/min) | $\emptyset_{OH^-}$ (ml/min) | $\emptyset_{residual\ CO_2}$ (ml/min) | $CO_2$ utilization rate (%) |
|---|---|---|---|---|---|
| 150 | 0.776 | 0.301 | 3.393 | 40.53 | 24.1 |
| 200 | 0.908 | 0.357 | 4.055 | 39.68 | 23.8 |
| 250 | 1.212 | 0.411 | 4.767 | 38.61 | 25.4 |
| 300 | 1.399 | 0.48 | 5.344 | 37.777 | 26.0 |

($\emptyset_{CO_2\ to\ gas}$: the consumed $CO_2$ flowrate which is electrochemcially converted into all gas products (CO, $C_2H_4$ and $CH_4$); $\emptyset_{CO_2\ to\ liquid}$: the consumed $CO_2$ flowrate for electrocatalytic reduction to all liquid products (such as ethanol and formate); $\emptyset_{OH^-}$: the consumed $CO_2$ flowrate via the reaction with $OH^-$; $\emptyset_{residual\ CO_2}$: the unreacted $CO_2$ (residual $CO_2$) flowrate in the gas outlet (gas mixture) after reactor.)

**Electrochemical impedance spectroscopy measurement**

To determine the solution resistance (Rs) in this work, potentiostatic electrochemical impedance spectroscopy (PEIS) was performed on Cu deposited GDE in a three-compartment flow electrolyzer at room temperature and atmospheric pressure.[5] During the experiments, the gas flow compartment was continuously fed with $CO_2$ at a flow rate of 45 ml/min. The impedance spectra were recorded using a potentiostat (Biologic) in the frequency range from 200 kHz to 10 mHz with an amplitude of 10 mV at fixed potentials. It should be noted that the variations in local ion species and concentration near surface of cathode at high-rate cathodic

reactions could make the local reaction environment complicated, and also lead to a distinct conductivity near cathode at high current densities compared to the measured results by PEIS. Even if a very tiny difference in resistance, a very high current could lead to an un-negligible variation in IR-corrected potentials. Thus, while the fixed distance between reference and cathode was less than 2 mm in this work, it is still difficult to get the accurate cathode potentials at relatively high current densities (for instance, the IR-corrected potentials at 300 mA/cm$^2$ in Table S3).

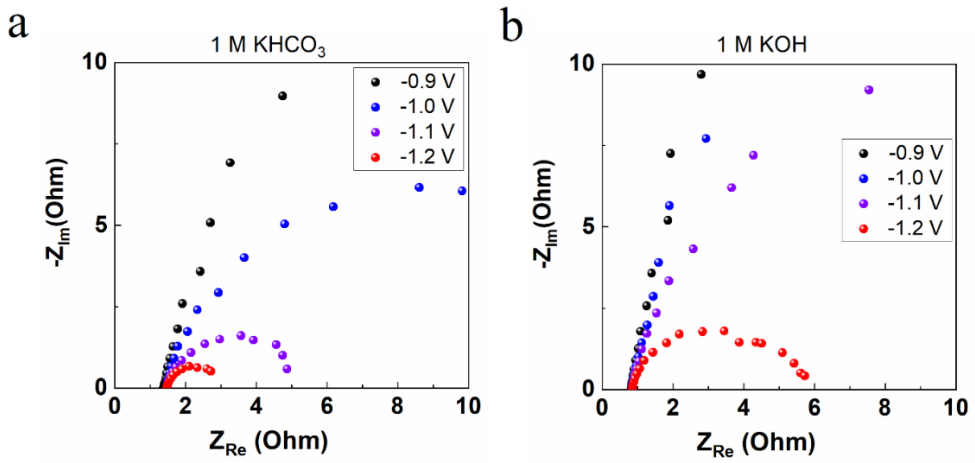


Figure S13. Nyquist plots of Cu deposited GDE in 1 M $KHCO_3$ aqueous solution (a) and 1 M KOH aqueous solution (b) at various potentials.

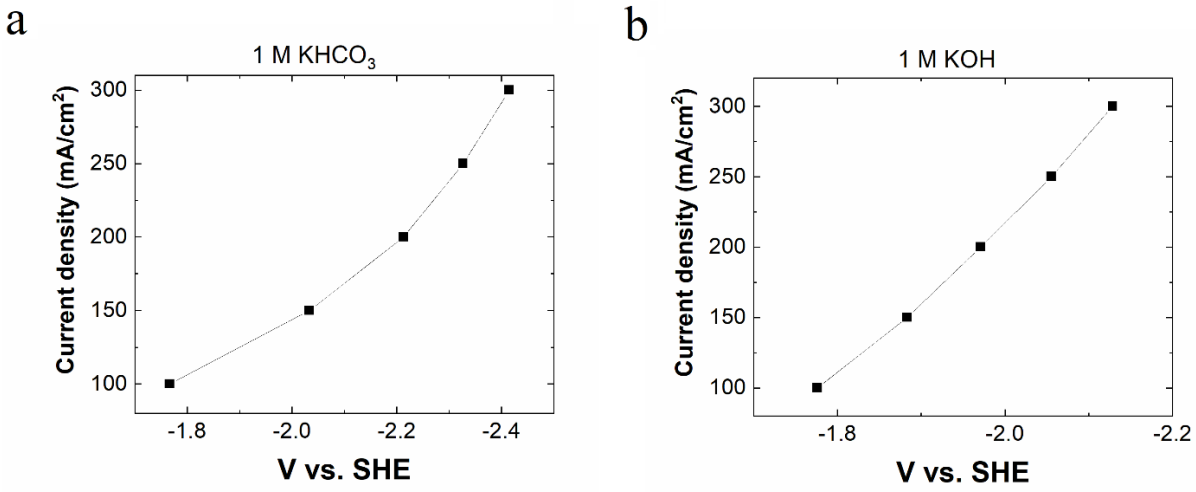


Figure S14. Current densities as a function of potential in 1 M $KHCO_3$ aqueous solution (a) and 1 M KOH aqueous solution (b) (The potentials were not IR-corrected).

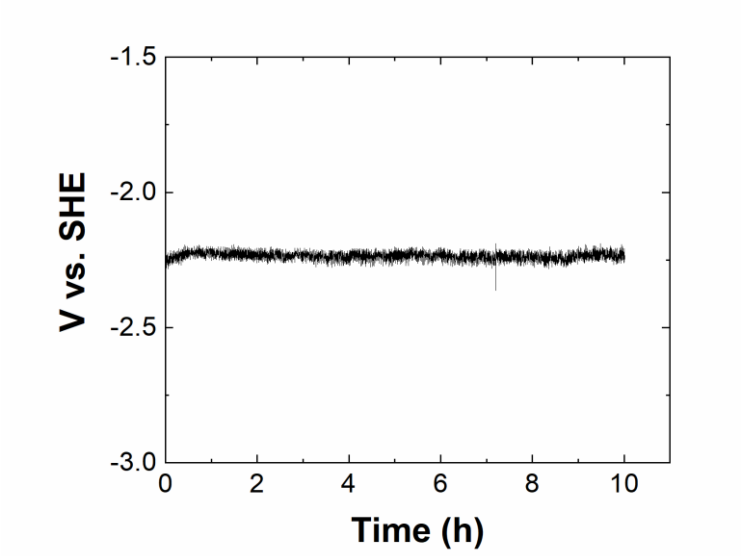


Figure S15. Applied potentials as a function of time at 200 mA/cm$^2$ in 1 M $KHCO_3$ electrolyte.

**Table S3**. IR-corrected potentials in 1 M KOH

| Current (mA) | R (Ω) | Corrected V vs. SHE |
|---|---|---|
| 200 | 0.82 | -1.61238 |
| 300 | 0.82 | -1.6375 |
| 400 | 0.82 | -1.64313 |
| 500 | 0.82 | -1.6455 |
| 600 | 0.82 | -1.648 |

**Table S4**. IR-corrected potentials in 1 M $KHCO_3$.

| Current (mA) | R (Ω) | Corrected V vs. SHE |
|---|---|---|
| 200 | 1.38 | -1.535 |
| 300 | 1.38 | -1.6075 |
| 400 | 1.38 | -1.63 |
| 500 | 1.38 | -1.6425 |
| 600 | 1.38 | -1.595 |

**Liquid products**

After completion of $CO_2$ reduction electrolysis, liquid-phase products were analyzed by a high-performance liquid chromatography (not in-situ analysis). In this work, both catholyte and anolyte in the given reservoirs were collected for quantification of liquid products due to that a part of liquid products transported from catholyte to anolyte via AEM (Figure S16). Here, the crossover ratio of one certain liquid product formed on cathode via AEM can be calculated according to the below equation:

$$Crossover\ ratio\ (\%) = \frac{N_{liquid\ in\ anolyte}}{N_{liquid\ in\ anolyte} + N_{liquid\ in\ catholyte}} \times 100\% \qquad (S15)$$

where $N_{liquid\ in\ anolyte}$ and $N_{liquid\ in\ catholyte}$ are the amount of one certain liquid product detected in anolyte and catholyte, respectively. Thus, the above equation can be used to calculate a ratio between the amount of one certain liquid product crossed to anolyte through AEM and the total amount of corresponding liquid product generated on cathode.

It should be noted that the volume of catholyte and anolyte slightly varied after about 2.5 h electrolysis (catholyte volume slightly decreased with increased anolyte), due to the anion species hydrated with water molecules transport from catholyte to anolyte via AEM as charge carriers. Thus, for getting accurate selectivity of liquid products in this study, we also measured volume of catholyte and anolyte after electrolysis, respectively.

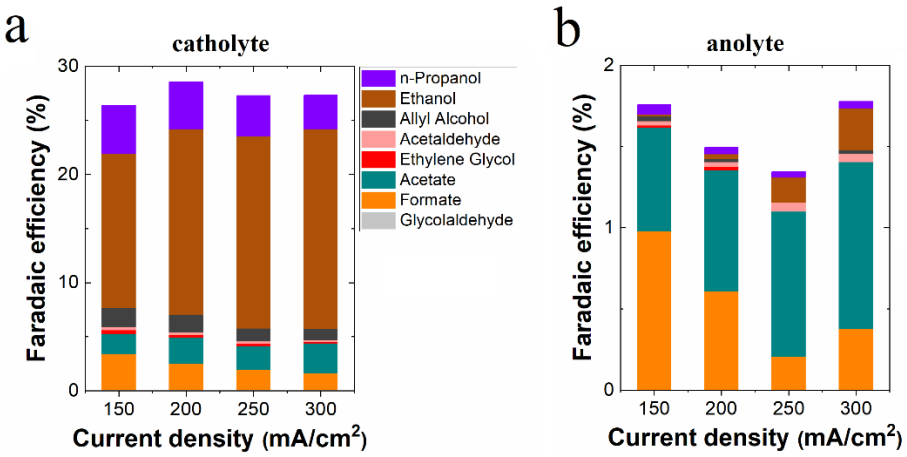


Figure S16. Faradaic efficiencies for all detected liquid products based on catholyte (a) and anolyte (b) in 1 M $KHCO_3$ at various current densities, respectively.

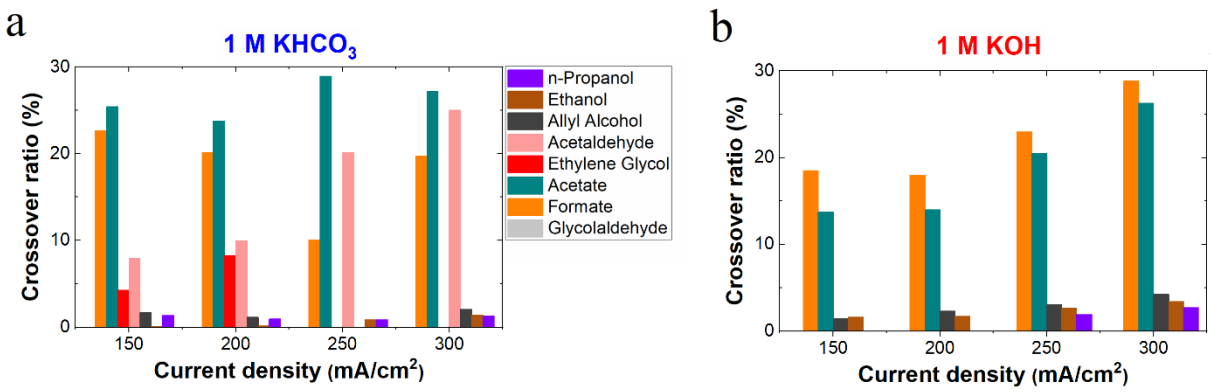


Figure S17. Crossover ratio of liquid products via AEM in 1 M $KHCO_3$ (a) and I M KOH (b) during about 2.5 h $CO_2$ reduction at various current densities, respectively.

**Table S5**. Faradaic efficiencies for liquid products in 1 M $KHCO_3$.

| J ($mA/cm^2$) | Glycolaldehyde (%) | Formate (%) | Acetate (%) | Ethylene Glycol (%) | Acetaldehyde (%) | Allyl Alcohol (%) | Ethanol (%) | n-propanol (%) |
|---|---|---|---|---|---|---|---|---|
| 150 | 0.0982 | 4.321 | 2.504 | 0.325 | 0.335 | 1.7733 | 14±0.3 | 4.511 |
| 200 | 0.1163 | 3.023 | 3.143 | 0.266 | 0.3 | 1.625 | 17.2±0.86 | 4.382 |
| 250 | 0.1322 | 2.042 | 3.0953 | 0.189 | 0.3 | 1.206 | 17.9±0.88 | 3.756 |
| 300 | 0.0958 | 1.906 | 3.790 | 0.152 | 0.21 | 1.0499 | 18.74±0.9 | 3.132 |

**Table S6**. Faradaic efficiencies for liquid products in 1 M KOH.

| J ($mA/cm^2$) | Glycolaldehyde (%) | Formate (%) | Acetate (%) | Ethylene Glycol (%) | Acetaldehyde (%) | Allyl Alcohol (%) | Ethanol (%) | n-propanol (%) |
|---|---|---|---|---|---|---|---|---|
| 150 | 0.8 | 3.705 | 2.871 | 0.25 | 0.56 | 1.5 | 16.74±0.87 | 4.5 |
| 200 | 0.6 | 2.1 | 2.8843 | 0.1404 | 0.26 | 1.105 | 19.7± 0.95 | 3.61 |
| 250 | 0.504 | 2.1 | 1.7735 | 0.11 | 0.25 | 1.1 | 18.44±0.88 | 3.84 |
| 300 | 0.462 | 1.9 | 2.581 | 0.11 | 0.7 | 1 | 18.4±0.2 | 3.04 |

**Effect of $CO_2$ inlet flowrate**

Effect of $CO_2$ inlet flowrate on the evaluation of Faradaic efficiencies for gas products in flow electrolyzers with and without the consideration of $CO_2$ consumption was explored in 1 M KOH electrolyte at 300 mA/cm$^2$. With decreasing the $CO_2$ inlet flowrate, gas products concentration in the gas chamber of the reactor enhanced significantly such as the detected CO concentration in Table S4.

**Table S7**. Detected CO concentration by GC under different $CO_2$ inlet flowrates in 1 M KOH electrolyte at 300 mA/cm$^2$.

| $CO_2$ inlet flow (ml/min) | CO concentration in the gas compartment of reactor (%) |
|---|---|
| 45 | 1.722336 |
| 30 | 2.85054 |
| 20 | 4.219992 |
| 15 | 5.45034 |

Without considering the $CO_2$ consumption (using uncorrected flow), the Faradaic efficiencies of gas products can be overestimated. Here, we defined the overestimation ratio of catalytic selectivity (only for gas products) without $CO_2$ consumption consideration by the following equation:

$$Overestimation\ ratio\ (\%) = \frac{FE_{inlet\ flow} - FE_{outlet\ flow}}{FE_{outlet\ flow}} \times 100\% \qquad (S16)$$

where, $FE_{outlet\ flow}$ and $FE_{inlet\ flow}$ are the Faradaic efficiency of gas product with and without the consideration of $CO_2$ consumption, respectively. After considering the calculation equation S2 for Faradaic efficiency of gas product, the equation S16 can be rewritten as:

$$Overestimation\ ratio\ (\%) = \frac{\emptyset_{inlet} - \emptyset_{outlet}}{\emptyset_{outlet}} \times 100\% \qquad (S17)$$

Where, $\emptyset_{inlet}$ and $\emptyset_{outlet}$ are the $CO_2$ inlet flowrate before reactor and a gas mixture outlet flowrate after reactor, respectivley. Thus, we got the overestimation ratio as a function of $CO_2$ inlet flowrate in 1 M KOH electrolyte at 300 mA/cm$^2$, as shown in Figure S18.

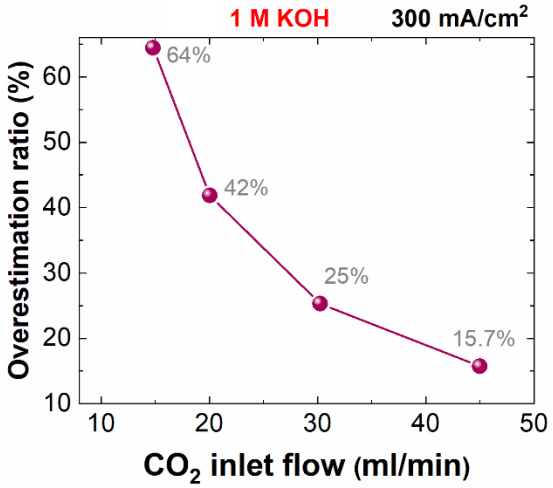


Figure S18. Overestimation ratio of gas product selectivity without $CO_2$ consumption consideration as a function of $CO_2$ inlet flowrate in 1 M KOH electrolyte at 300 mA/cm$^2$.

REFERENCES

(1) Kuhl, K. P.; Hatsukade, T.; Cave, E. R.; Abram, D. N.; Kibsgaard, J.; Jaramillo, T. F. Electrocatalytic Conversion of Carbon Dioxide to Methane and Methanol on Transition Metal Surfaces. *Journal of the American Chemical Society* **2014**, *136* (40), 14107–14113.

(2) Hori, Y. Electrochemical $CO_2$ Reduction on Metal Electrodes. In *Modern Aspects of Electrochemistry*; Vayenas, C. G., White, R. E., Gamboa-Aldeco, M. E., E., Ed.; Springer New York: New York, NY, 2004; Vol. 70, pp 89–189.

(3) Ma, M.; Djanashvili, K.; Smith, W. A. Controllable Hydrocarbon Formation from the Electrochemical Reduction of $CO_2$ over Cu Nanowire Arrays. *Angewandte Chemie International Edition* **2016**, *55* (23), 6680–6684.

(4) Dinh, C.-T.; Burdyny, T.; Kibria, M. G.; Seifitokaldani, A.; Gabardo, C. M.; García de Arquer, F. P.; Kiani, A.; Edwards, J. P.; De Luna, P.; Bushuyev, O. S.; et al. $CO_2$ Electroreduction to Ethylene via Hydroxide-Mediated Copper Catalysis at an Abrupt Interface. *Science* **2018**, *360* (6390), 783–787.

(5) Kibria, M. G.; Dinh, C. T.; Seifitokaldani, A.; De Luna, P.; Burdyny, T.; Quintero-Bermudez, R.; Ross, M. B.; Bushuyev, O. S.; García de Arquer, F. P.; Yang, P.; et al. A Surface Reconstruction Route to High Productivity and Selectivity in $CO_2$ Electroreduction toward $C_{2+}$ Hydrocarbons. *Advanced Materials* **2018**, *30* (49), 1804867.